EXTRATROPICAL SECONDARY CYCLONES: SIMULATIONS AND OBSERVATIONS

M. A. SHAPIRO[1*], JIM DOYLE[2], XIAOLEI ZOU[3], and DAVID P. JORGENSEN[4]
[1]NOAA/ERL/Environmental Technology Laboratory, Boulder CO, [2]Naval Research Laboratory, Monterey CA,
[3]Florida State University, Tallahassee FL, [4]NOAA/National Severe Storm Laboratory, Boulder CO; USA

1997

1. INTRODUCTION

Extratropical cyclones are observed over a broad spectrum of spatial scales: synoptic-scale primary cyclones (~4,000 km), intermediate-scale secondary frontal-wave cyclones (~1000 km), and the lesser mesoscale cyclones (~500-100 km). The fundamental difference between primary and secondary cyclones was described by Eliassen (1966): *"A natural conclusion from the various theories is that the large-scale cyclonic systems associated with the transient waves in the upper-westerlies are the primary perturbation systems, since their existence can be accounted for by baroclinic instability, even in the absence of fronts. These large cyclonic systems, in turn, produce the fronts, partly by setting up the deformation fields required in Bergeron's theory, and partly by the non-linear process demonstrated by Edelmann. Finally, the fronts will give birth to the smaller, frontal wave [secondary] cyclones".*

This paper addresses two categories of sub-synoptic-scale cyclones: i) secondary cyclones that form through upstream baroclinic development (see, e.g., Simmons and Hoskins 1979) at the end of the trailing cold fronts of the primary synoptic-scale cyclones, in the absence of an initial localized disturbance in the vicinity of the tropopause; ii) intermediate- scale and mesoscale cyclones that form along the occluded bent-back warm fronts of primary cyclones. Selected examples of these categories of secondary cyclones are illustrated with numerical simulations and case study observational verifications.

2. THE UPSTREAM SECONDARY CYCLONE DEVELOPMENT OF 15-16 FEBRUARY 1997

Figure 1 presents the satellite cloud-images of the life cycle of a North-Atlantic primary cyclone and its associated upstream secondary cyclone development observed in the period 14-16 February 1997 during the field phase of the Fronts and Atlantic Storm-Track Experiment (FASTEX). At 0000 UTC 14 February 1997, the incipient phase of a primary North-Atlantic cyclone was centered south-east of Newfoundland, identified as Low 38 of FASTEX. The satellite mosaic (Fig. 1a), shows the developed cloud 'head' of the incipient of primary Low 38 east of Newfoundland, with it center located near the cloud-free 'notch' at eastern edge of the cloud head. By 0000 UTC 15 February (Fig.1b), Low-38 had undergone rapid intensification over the central-North Atlantic and by 0000 UTC 16 February (Fig. 1c), had entered its occlusion phase east of Ireland. At this time, the cloud imagery (Fig. 1c) shows the bright

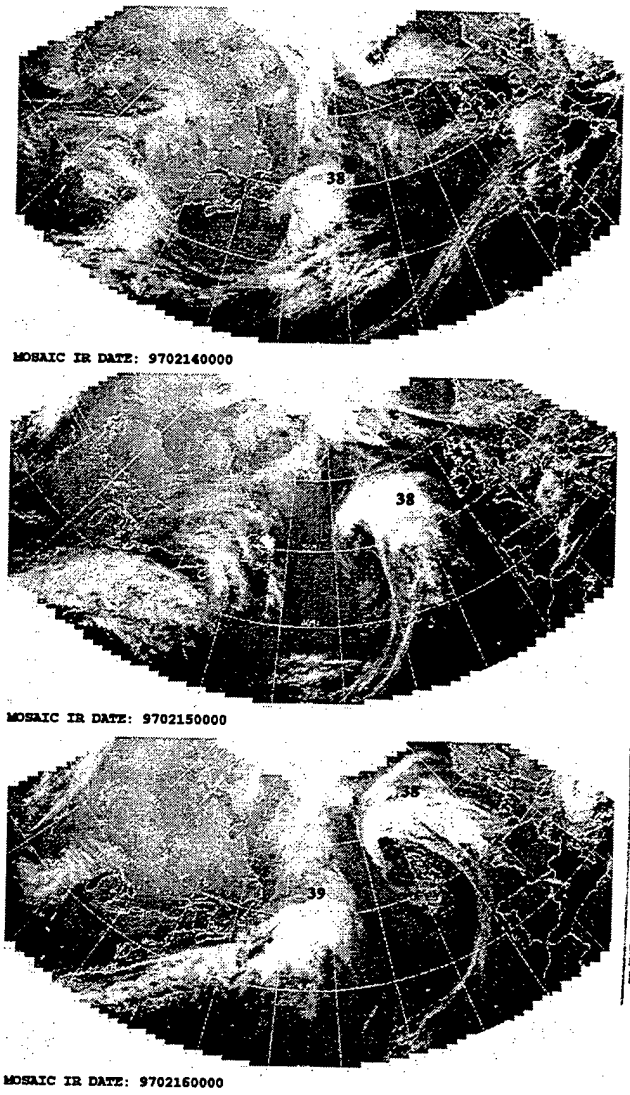

Figure 1. GOES-9 and METEOSAT infra-red mosaic for the period 14-16 February 1997.

(cold) cloud 'head' east of Newfoundland associated with the first of two upstream secondary cyclone developments. The first upstream development (Low 39) formed in the same location in as where the primary cyclone (Low 38) was born two days earlier (Fig. 1a).

A numerical simulation of this situation was performed with the NCAR/Penn State, MM-5 model configured with full physics, a horizontal resolution of 40 km and 23 vertical levels; initialized at 1200 UTC 15 February 1997. from the National Centers for Environmental Prediction (NCEP) global analysis. At 1200 UTC 15 February, the mature primary cyclone (Low 38) was centered west of Ireland and its associate high was positioned east of Cape Hatteras, North Carolina (Fig. 2a). This low/high pressure dipole represents the surface signature of a fully developed synoptic-scale primary baroclinic development. We draw attention to the ~20 ms^{-1} southwesterly low-level jet flow

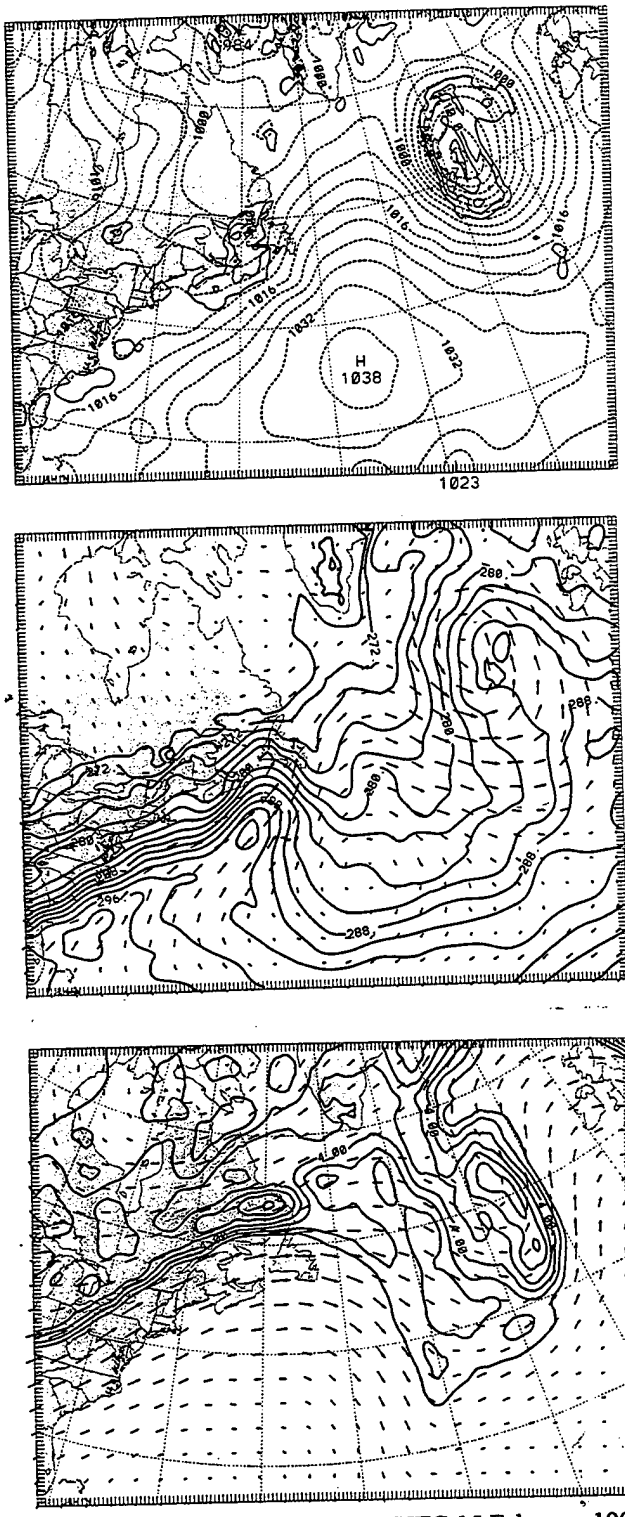

Figure 2. Initial conditions at 1200 UTC 15 February 1997. (a) sea-level pressure (mb, dashed lines), 950-mb relative vorticity (solid lines); (b) 950-mb potential temperature (K, solid lines) and wind vectors; (c) 320-K potential vorticity (PVU, solid lines and wind vectors).

and substantial warm advection within the baroclinicity of thermal ridge at the western flank of the mid-Atlantic anticyclone southeast of Newfoundland (Fig. 2b). This thermal ridge formed on the trailing (weakening) cold front of Low 38 which had become aligned with the baroclinicity of the Gulf stream off the eastern shore of North America. The crest of the thermal ridge contains characteristics considered as first-order components in the initiation of surfaced-based secondary frontal-wave cyclones: i) localized warm advection which contributes to thermal wave amplification and positive boundary-PV development; ii) vorticity generation through vortex stretching (convergence) as inferred from the speed convergence in the absence of compensating directional difluence south of Newfoundland; iii) latent heating through condensation in the region of maximum warm advection; iv) upward sea-surface fluxes of latent and sensible heat into the wave warm sector. From a PV perspective (see e.g., Thorncroft and Hoskins 1990), the southwesterly flow in the crest of the upstream thermal ridge is attributable to the negative (cold) boundary PV anomaly of the primary baroclinic development to the east.

At 1200 UTC 15 February, the potential vorticity (PV) analysis and wind vectors on the 320-K isentropic surface (Fig.2c), shows the large-amplitude, synoptic-scale (~4,000 km) tropopause PV wave, with Low 38 centered beneath the positive PV anomaly of the wave trough. The lower-tropospheric thermal ridge of the incipient upstream baroclinic development (Fig. 2b) is found beneath the anticyclonic (negative) PV anomaly of the synoptic-scale ridge aloft and >500 km south of the upper-level jet-stream axis and its associated PV gradient zone and tropopause fold (Fig. 2c). Since there is no signature of an intermediate-scale cyclonic PV anomaly in the vicinity of the western-Atlantic frontal wave, it is unlikely that tropopause PV anomaly attribution significantly contributed to the initiation of this upstream baroclinic development.

The 24-h MM-5 simulation of sea-level pressure and 950-mb relative vorticity at 1200 UTC 16 February (Fig. 3) shows the well developed Low 39 secondary cyclone off the southern tip of Greenland, midway between the occluded, decaying primary Low 38 to its northeast and a new upstream frontal wave development off the eastern shore of North America.

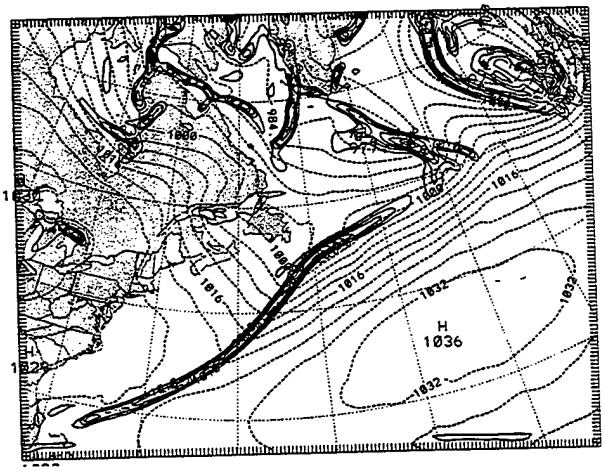

Fig 3. Simulated seal-level pressure and 950-mb relative vorticity at 1200 UTC 16 February 1997 (lines as in Fig. 2)

Dynamical confirmation for the interpretation of thi upstream secondary cyclogenesis was diagnosed throug sensitivity calculations with the dry adjoint of MM- developed by Zou et al. (1997). Results reveal that th initiation of the upstream secondary frontal wave of 120 UTC 15 February was most sensitive to the primar baroclinic development that began 36 hrs prior to th formation of the secondary frontal wave within the sam region. There was little sensitivity to any transient P

anomaly approaching from the west prior in the initiation of the Low 39 secondary cyclone.

3. SUBSYNOPTIC-SCALE CYCLONES WITHIN FASTEX IOP--18

During FASTEX a variety of extratropical cyclones were investigated with research aircraft which included the NOAA P-3 equipped with a side-scanning airborne Doppler radar, and UK Met. Service C-130 and NOAA/G-IV which deployed high-resolution dropwindsondes. The measurements from these aircraft documented the wind, thermodynamic and precipitation structure of subsynoptic-scale (mesoscale) cyclones of 100 km to 400- km diameter that formed along a bent-back warm-frontal occlusion of the synoptic-scale cyclone development of 23-25 February 1997, identified as IOP-18 of FASTEX. The characteristics of these mesoscale cyclones are compared to results of their numerical simulation with the Naval Research Laboratory COAMPS multi-scale prediction model (Hodur 1997).

Figure 4 illustrates ~100-km-scale meso-cyclones along the bent-back warm front of the FASTEX/IOP-18 cyclone at 1515 UTC 23 Febuary 1997. Figure 5 presents the satellite cloud imagery at 1839 UTC 24 February of the decaying phase of an internal ~400 km scale mesoscale cyclone at the center of the IOP-18 cyclone west of the UK.. A maturing phase of a second mesoscale cyclone is seen between Iceland and Norway. These features were documented with research aircraft measurements and simulated with the COAMPS model.

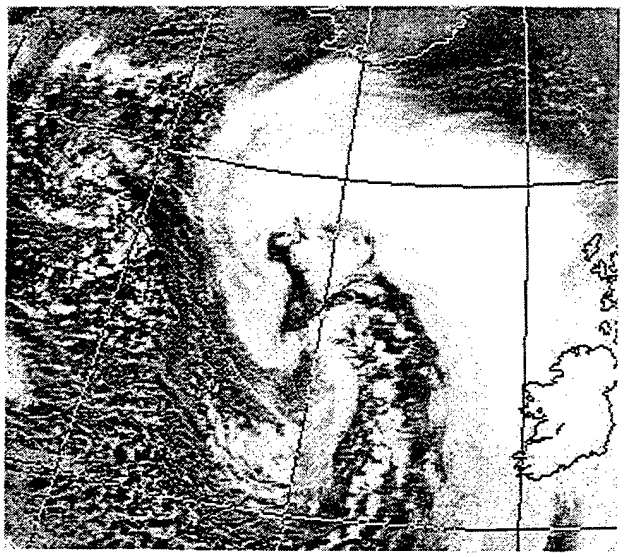

Fig.4. NOAA polar orbiter satellite infra-red cloud imagery at 1839 UTC 23 February 1997.

The COAMPS simulation of the dual cyclones in Fig. 4., verifying at 1500 UTC 24 February 1997 is shown in Fig 6. For this simulation, the model was configured with a horizontal resolution of 15 km and 30 levels, and nested within the coarser resolution NRL/NOGAPS global model. The simulation has successfully reproduced structures inferred from the satellite imagery, above; such as the mesoscale cyclonic development between Iceland and Norway that formed along the low-level vorticity filament of the parent cyclone bent-back warm front (Fig. 5).

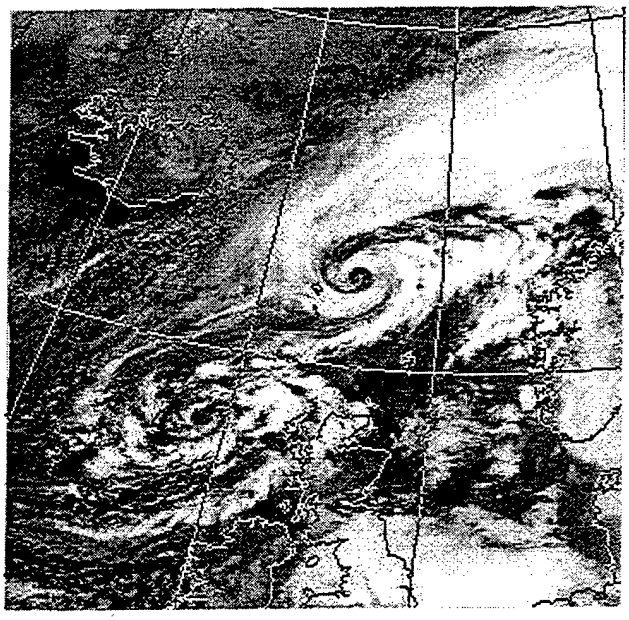

Fig. 5. Same as Fig. 4, but for 1839 UTC 24 February 1997.

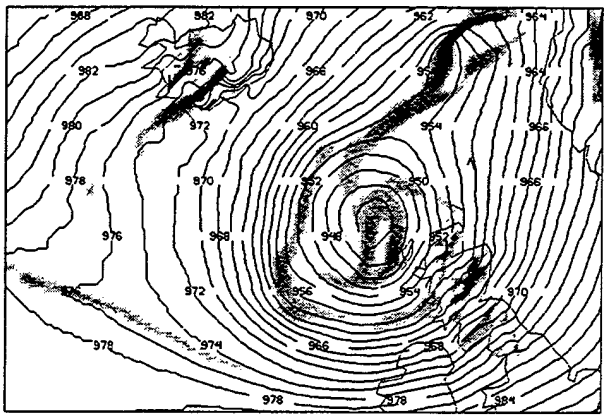

Fig. 6. NRL/COAMPS 27-hr forecast valid at 1500 UTC 24 February 1997. Sea-level pressure (mb, solid lines); absolute vorticity (>10^{-4} s^{-1}, shaded).

4. REFERENCES

Eliassen, A., 1966: Motions of intermediate scale: fronts and cyclones. *Advances in Earth Science.*, E.D Hurley, Ed., The MIT Press, 111-138.

Hodur, R.M., 1997: The Naval Research Laboratory's Coupled Ocean/Atmosphere Mesoscale Prediction System (COAMPS). *Wea Mon. Rev.*, **125**, 1414-1430.

Simmons, A. J., and B. J. Hoskins, 1979: The down-stream and upstream development of unstable baroclinic waves. *J. Atmos. Sci.*, **36**, 1239-1254.

Thorncroft, C. D., and B. J. Hoskins, 1990: Frontal Cyclogenesis. *J. Atmos. Sci*, **47**, 2317-2336.

Zou, X., F. Van Den Berghe, M. Pondeca, and Y.-H. Kuo, 1997: Introduction to adjoint techniques and the MM5 adjoint modeling system. NCAR/TN-435-STR, 110pp.